Methods in Ecology and Evolution

British Ecological Society

Methods in Ecology and Evolution 2015, **6,** 1190–1198 doi: 10.1111/2041-210X.12396

A method for identifying Sound Scattering Layers and extracting key characteristics

Roland Proud[1,2,3]*, Martin J. Cox[2], Simon Wotherspoon[2,3] and Andrew S. Brierley[1]

[1]*Pelagic Ecology Research Group, Scottish Oceans Institute, University of St Andrews,St Andrews KY16 8LB, UK;* [2]*Australian Antarctic Division, 203 Channel Highway, Kingston, Tas. 7050, Australia; and* [3]*Institute of Marine and Antarctic Studies, University of Tasmania, 20 Castray Esplanade, Battery Point, Hobart, Tas. 7004, Australia*

Summary

1. Mid-trophic level water-column (pelagic) marine communities comprise millions of tonnes of zooplankton and micronekton that form dense and geographically extensive layers, known as sound scattering layers (SSLs) when observed acoustically. SSLs are ubiquitous in the global ocean, and individual layers can span entire ocean basins. Many SSLs exhibit clear diel vertical migration behaviour. Vertical migrations contribute substantially to the 'biological pump', such that SSLs have important global biogeochemical roles: SSLs are important conduits for vertical energy and nutrient flow. Ship-based remote sensing of SSLs using acoustic instruments (echosounders) enables their shape and density to be quantified, but despite SSLs being discovered in the 1940s, there is no consistent method for identifying or characterising SSLs. This hampers ecological and biogeographical studies of SSLs.

2. We have developed an automated and reproducible method for SSL identification and characterisation, the sound scattering layer extraction method (SSLEM). It functions independently of echosounder frequency and the spatial scale (vertical and horizontal) of the data. Here we demonstrate the SSLEM through its application to identify SSLs in data gathered to a depth of 1000 m using 38 kHz hull-mounted echosounders in the south-west Indian Ocean and Tasman Sea.

3. SSLs were identified in the water column as horizontally extensive echoes that were above background noise. For each identified SSL, a set of 9 quantitative 'SSL metrics' (describing their shape, dynamics and acoustic backscattering distribution) were determined, enabling inferences to be made concerning the spatial arrangement, distribution and heterogeneity of the biological community. The method was validated by comparing its output to a set of visually derived SSL metrics that were evaluated independently by 8 students. The SSLEM outperformed the by-eye analysis, identifying three times the number of SSLs and with greater validity; 95% of SSLs identified by the SSLEM were deemed valid, compared to 75% by the students.

4. In the same way that data obtained from satellites have enabled the study and characterisation of global phytoplankton distribution and production, we envisage that the SSLEM will facilitate robust, repeatable and quantitative analysis of the growing body of SSL observations arising from underway-acoustic observations, enhancing our understanding of global ocean function.

Key-words: biological communities, biological layers, deep scattering layers, diel vertical migration, marine acoustics, mid-trophic level, pelagic ecology, sound scattering layer extraction method, SSL metrics

Introduction

Sound scattering layers (SSLs) or deep scattering layers (DSLs) are vertically discrete (100s of m or less) water-column aggregations of organisms that can extend horizontally over 1000s of km (Kloser *et al.* 2009). The layers are comprised of pelagic organisms (organisms of the water column, as opposed to benthic organisms that live on or in the seabed), primarily zooplankton and small fish (cm to 10s cm), living together in distinct communities. When insonified, these organisms produce a distinct echo that, depending upon depth and incident acoustic frequency, can stand out prominently as scattering layers above background noise (Simmonds & MacLennan 2005). Such layers have been known since the mid-20th century when naval sonars detected signals thought initially to be echoes from the sea bed: the depths of the echoes, however, changed with time of day and it became apparent that these 'false bottoms' were in fact biological in origin (Brierley 2014).

The organisms that comprise SSLs are responsible for the transport of vast quantities of carbon (increasing particle export by up to 40% – Bianchi *et al.* 2013) from the surface to the deep sea (the biological pump) via diel vertical migration (DVM), the largest known daily migration of biomass on the planet (Hays 2003). They thus play an important role in

*Correspondence author. E-mail: rp43@st-andrews.ac.uk

atmosphere–ocean interactions and in the global biogeochemical cycle. SSL scales can vary from the micro, at vertical resolutions of centimetres over time-scales of a fraction of a minute (Holliday *et al*. 2003; McManus *et al*. 2003, 2005) to pan-oceanic (Anderson, Brierley & Armstrong 2004; Kloser *et al*. 2009; Irigoien *et al*. 2014). The former, so-called microlayers provide an explanation for the 'paradox of the plankton' where high species diversity occurs in what at first glance may appear to be a homogenous volume of water. Vertical structure means that the water column is in fact far from homogenous. Its physical properties can change dramatically over just a few centimetre's or metres enabling the discrete formation of aggregates at specific depth ranges (Longhurst 1998). In this way, SSLs show the water column divided into multiple vertically discrete habitats. Despite the importance of SSLs to ocean and earth-system function, there is no accepted standard method for identifying or classifying them. This in turn has hampered comparative or integrative studies of SSLs.

There are parallels between the pelagic and tropical rain forest ecosystems, in as far as both have vertical layered structure that with increasing depth is increasingly light limited. The sea surface, like the forest canopy, can be studied remotely by satellites and yield estimates of biomass and primary production (PP) (Longhurst, 1998). The sea bed is a physically fixed entity, and organisms living there, like organisms and vegetation of the forest floor, are amenable to study because they are constrained by a two-dimensional environment. The ocean interior, however, is physically dynamic, and its inhabitants – pelagic organisms including zooplankton and fish – have freedom to move in three dimensions, so the dynamics of the sometimes-dense layers of mid-trophic level communities are poorly understood (Lehodey, Murtugudde & Senina 2010). Developments in forest sampling can perhaps guide developments in ocean sampling.

In an effort to improve understanding of rain forest interiors, the 'RAINFOR' project (Malhi *et al*. 2002) that was established over a decade ago initialised a network of sampling sites for Amazonian rain forest ecosystems. As part of the initiative, field measurements of the forest interior were taken and the data related back to satellite information in order to gain a more complete picture of the ecosystem and to provide the capability to validate remotely sensed data. Since the rain forest covers <7% of the earth's surface (Bierregaard *et al*. 1992; Wilson 1994), a network of sites can provide a representative sample. The ocean on the other hand covers over 71% of the earth's surface and therefore makes it extremely difficult, logistically and financially to study the pelagic community by *in situ* biological sampling alone. The required greater spatial coverage for the ocean can be achieved by using active acoustic sampling techniques (scientific echosounding) to rapidly observe large volumes of the ocean, from ship-based instruments routinely used on both research and fishing vessels. These acoustic data can help reveal the spatial structure of pelagic communities: many marine organisms scatter sound waves in a characteristic fashion (dependant on the frequency of the incident wave and anatomy of the organism) such that 'remote sensing' by echosounder can provide community insight. These data could then be linked back to remotely sensed PP data at the surface, acquired from online resources such as the National Oceanographic Data Centre (NODC, www.nodc.noaa.gov) and validated by biological point samples, available from, for example, the Ocean Biogeographical Information System (OBIS, www.iobis.org). Acoustic survey data already exist in vast quantities, with wide geographic coverage, leading to the possibility that a method capable of identifying and characterising pelagic communities, found within SSLs, would, akin to the RAINFOR project, potentially enable deep ocean processes to be inferred from satellite observation of the surface, yielding a more complete understanding of ocean ecosystem function. To achieve this, first a repeatable technique to identify and parameterise SSLs is required.

Some quantitative research has already been carried out on SSLs. Regional structure of SSLs has been identified by comparing total water-column backscattering strength at sites across the Pacific and Atlantic Oceans, in the Caribbean, Labrador, Norwegian and Mediterranean Seas and in Baffin Bay (Chapman *et al*. 1974) and also in the Atlantic and north-western Pacific using depth-frequency structure of backscattering strength (Andreeva, Galybin & Tarasov 2000; Tarasov 2002). Biomass estimates of SSLs have also been made at the basin scale using both echo counting and echo integration techniques, in the Tasman Sea, for example (Kloser *et al*. 2009). More recently, a method was developed to extract SSLs (Cade & Benoit-Bird 2014) that required input parameters such as an acoustic threshold intensity and minimum separation distances between SSLs to be defined *a priori*.

Research on SSLs has, however, typically been qualitative. The depth structure of SSLs has been observed to vary over large spatial scales in both longitude and latitude (Kloser *et al*. 2009), across ocean basins (Anderson, Brierley & Armstrong 2004) in the Irminger Sea and across fronts (Nicol *et al*. 2000; Kawaguchi *et al*. 2010) in the southern Ocean. Studies at oceanic features have also shown characteristic behaviour, such as bulges in SSLs at continental shelves (Jarvis *et al*. 2010) off East Antarctica and bowl-like SSL features forming under eddy structures (Godø *et al*. 2012) in the Norwegian Sea.

Conversely, discrete, biological aggregations – schools, shoals and swarms – have been quantitatively defined. The fisheries acoustic community has wrestled for years over the question of what, as seen in an acoustic record, is a school, and some standard identification and description protocols have been agreed (Reid & Simmonds 1993; Reid 2000). The importance of particular school metrics for school identification has differed between studies; for example, Coetzee (2000), using the Shoal Analysis and Patch estimation system algorithm (SHAPES: Barange *et al*. 1994), identified morphological aspects to be the chief descriptor; Lawson (2001) identified school energetics and water-column position as the most important parameters.

In spite of previous work, no standardised objective approach exists for defining SSLs, rendering comparisons between studies and between water-column communities and the environment difficult beyond the merely descriptive. The lack of a consistent analytical approach was identified by

Handegard *et al.* (2013) as hindering marine ecosystem monitoring and management.

Our overarching goal was to develop a standardised analysis method to extract biological layers consistently from underway-acoustic survey data. We illustrate the utility of our method here by identifying SSLs from data observed at 38 kHz in the south-west Indian Ocean and Tasman Sea. Application of this method will lead to a better understanding of mid-trophic level communities, within and across oceanic boundaries at varying spatial and temporal scales.

Materials and methods

ACOUSTIC DATA

The acoustic data used in this study were all 38 kHz data and were obtained from the Integrated Marine Observing System data centre (IMOS 2013, www.imos.au, downloaded on 1st June 2013). Thirty-eight kilohertz data were suitable for SSL observations because the moderately low attenuation rate (5–10 dB km^{-1}: Ainslie & McColm 1998) enables deep water-column penetration (up to 1500 m) and because the wavelength is appropriate for detection of many of the fish and plankton species of the order of centimetre's that inhabit the layers. Data had been collected by research vessels (RV) *Southern Surveyor* and *Aurora Australis*, as well as several fishing vessels (FVs) including the *Southern Champion*, *Janas*, *Rehua*, *Austral Leader II* and *Will Watch*. Data were granted by the Marine National Facility and processed by the Commonwealth Scientific and Industrial Research Organisation (CSIRO) Oceans and Atmosphere Flagship as part of the IMOS Bio-Acoustic Ships of Opportunity (BASOOP) Program. The data totalled 24 transects covering wide areas of the south-west Indian Ocean and Tasman Sea (Fig. 1). Transect length ranged from 200 to 1800 NM and included 24 h (day/night) coverage across all seasons between 2009 and 2012. The spatial coverage of the tracks included two of the four major global ocean biomes as described by Longhurst (1998) – the Trades and Westerlies – and also spanned major frontal zones and boundaries including the subtropical convergence zone (STCZ) and the polar front (PF).

We pre-processed IMOS data by removing dropped pings (a ping is a single acoustic transmit/receive cycle; typical ping rate was 0·5 Hz) and noise spikes (caused for example by violent ship's motion in rough seas) and partitioned data into separate day/night segments, bounded by sunrise/sunset. In instances where, for example, the echosounder had been turned off for short periods, or the vertical sampling resolution of the echosounder was changed, data were further segmented. An acoustic image, or echogram, was created for each segment. The acoustic image was defined as a two-dimensional array of backscatter values on a depth v time (or space) grid. Each cell in the image, an acoustic pixel, had an associated timestamp, geographical position and depth. For each image, echo intensity in the form of mean volume backscattering strength (MVBS – Simmonds & MacLennan 2005) was calculated at a cell resolution of 5 m in depth (from the surface down to 1000 m) by 1 min in time.

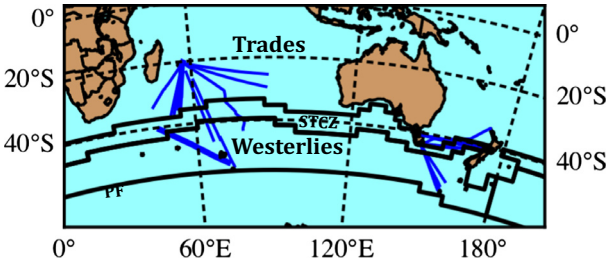

Fig. 1. Map showing ship transect lines (blue) for acoustic data extracted from the Integrated Marine Observing System (IMOS) data centre. Mean positions of the subtropical convergence zone (STCZ) and polar front (PF) are marked as well as two Longhurst Biomes, the Trades and the Westerlies, separated by the northern boundary of the STCZ.

SSL EXTRACTION METHOD (SSLEM)

Our objective was to provide a method that would function over the range of bio-acoustical echosounder frequencies in common (and likely future) use, over horizontal scales from bays to oceans, and on vertical scales that encompass microlayers (cm; Holliday *et al.* 2003) upwards to tens and hundreds of metres. The common observational frequency band (18–200 kHz) spans the Rayleigh and geometric scattering regions for most zooplankton and nekton. This means that small changes in frequency can result in large changes in backscattering intensity and hence in SSL descriptors. Layers only become apparent acoustically when they can be distinguished from background noise (sufficiently high signal-to-noise ratio – SNR). SNR is a function of organism packing density, acoustic target strength, depth, insonification frequency and power, and environmental conditions (Simmonds & MacLennan 2005). SSL appearance may also be influenced by sampling resolution (Korneliussen *et al.* 2008): for transect data resolution is determined by ping rate, beam angle, depth and ship speed. The geographic scale of data is an important consideration as there are many oceanic processes that occur over different spatial and temporal scales, from microturbulence to decadal oscillations. A robust general method should be capable of resolving features of interest at the scale of the study being conducted and for the organisms of interest in the environment in which they exist.

Identification of SSLs

The SSL extraction method (SSLEM) is based upon detection of a contrast in MVBS (Berge *et al.* 2014) between pixels within SSLs (relatively high MVBS signal) and background pixels outside (relatively low MVBS noise). For a simple SSL analysis, using a window of depth range Z and time/space extent X, one could identify a vertically 'static' SSL surrounded by empty water by selecting pixels for which MVBS intensities were greater than the mean, μ, over the entire window. Under such a scheme, for any acoustic pixel (px) within the analysis window,

$$ssl = \begin{cases} 1, & px > \mu \\ 0, & px \leq \mu \end{cases} \qquad \text{eqn 1}$$

where *ssl* is a Boolean variable, taking a value of 1 for pixels that are deemed to belong to an SSL and 0 for those that are not. This simple process, useful as an introduction to the method, assumes that the SSL is completely contained by the analysis window, and the surroundings are made up of pixels with low MVBS that is attributable to background noise. This may not be the case; for example, a transition between depth intervals that exhibit a difference in background noise (inherently caused by time-varied gain (TVG) amplification of background noise) would yield a layer-like boundary of *ssl* pixels. To ensure that SSLs were surrounded by lower intensity MVBS (both towards the surface and the seabed), the depth interval of the analysis window

was divided into two equal values, d_1 and d_2, and pixels were only deemed a SSL pixel (*ssl* value of 1) when their MVBS value was larger than both the MVBS means, μ_1 and μ_2, over each of the two regions of the split window (Fig. 2a), yielding a new equation for *ssl*:

$$ssl = \begin{cases} 1, & (px > \mu_1) AND (px > \mu_2) \\ 0, & otherwise \end{cases} \quad \text{eqn 2}$$

where μ_1 and μ_2 are calculated over the regions X by d_1 and X by d_2, respectively, and where d_1 is equal to d_2.

In practice, using a fixed analysis window does not capture all SSLs, since they are rarely vertically static: they may for instance oscillate with internal wave activity or migrate vertically. To accommodate this, an analysis column one pixel wide was used instead of a window. The column was moved pixel-by-pixel through the image evaluating the pixel at the centre of the column at each step, such that μ_1 and μ_2 were calculated over the specific column (single point in time series), not the entire window, bounded either side of the central pixel by the depth ranges d_1 and d_2. For constant values of d_1 and d_2, this approach would only work if all SSLs had the same thickness and were separated by distances larger than the size of d_1 or d_2: this is not the case. To overcome this problem, the depth ranges d_1 and d_2, for each pixel evaluated, were varied in size from two pixels in height (this minimum, rather than 1, was used to avoid flooding the image with incorrectly assigned *ssl* pixels when analysing highly variable or 'noisy' images) up to the vertical extents of the image (Fig. 2b). Then, for any pixel within an image evaluated using a dynamic column,

$$ssl = \begin{cases} 1, & \left(\sum_{d_1=2}^{r-1} \sum_{d_2=2}^{R-r} (px > \mu_1) AND (px > \mu_2) \right) > 0 \\ 0, & otherwise \end{cases} \quad \text{eqn 3}$$

where r is equal to the row number of the pixel being evaluated and R equal to the total number of rows within the image; consequently, the first and last two rows of each image are not processed. Each pixel thus has multiple opportunities (for varying d_1 and d_2 values) to be attributed an SSL pixel. This ensured that both vertically static and migrant SSLs of varying thicknesses and separation distances would all be identified.

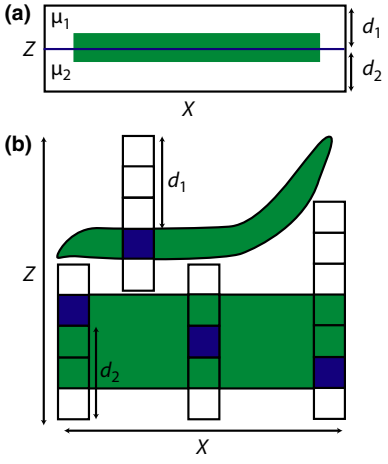

Fig. 2. Identification of sound scattering layer (SSL) pixels, where green features indicate relatively high intensity SSLs, white background indicates low intensity noise (or empty water) and blue cells represent the SSL pixel being evaluated. (a) Simple SSL analysis window: only vertically static SSLs separated by a distance larger than d_1 or d_2 are detected. (b) Dynamic SSL analysis column: a column is moved pixel-by-pixel through the image, where at each step the column size ranges from the minimum (5 pixels in length; where d_1 and d_2 are both equal to 2 pixels plus the pixel being evaluated) up to the full vertical extent of the Z axis, by stepping through all the possible values for each of the two parameters, d_1 and d_2; in doing so, SSLs of varying separation distances and vertical behaviours are captured.

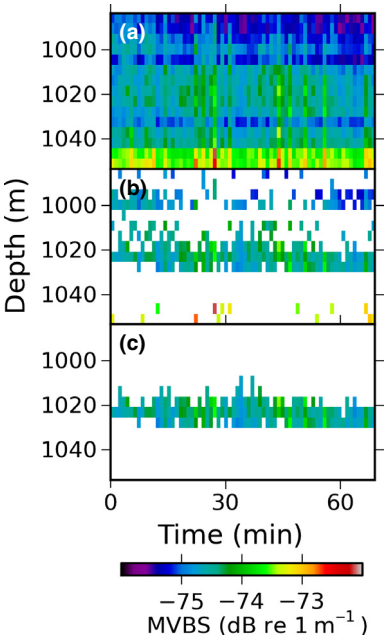

Fig. 3. Phantom sound scattering layer (SSL) extracted from FV *Austral Leader II* transect during May 2012, where SSL_{min}, the minimum horizontal resolution of SSLs, was set to 60 min (a) acoustic image segment. (b) SSL pixels identified by the method (section 'Identification of SSLs'). (c) Extracted phantom SSL: MVBS values of the SSL are similar to that of the surrounding background.

Phantom SSLs and SSL_{min}

On occasions when no SSL was present in the analysis column, pixels would sometimes erroneously be designated as SSL pixels as a result of the backscatter from individual or diffuse arrangements of organisms, tightly packed schools or swarms, variation of the physical properties of sea water, or by natural variation inherent within the data. The variable, SSL_{min}, which designated a fixed minimum horizontal extent for SSLs (measured in space/time units), was therefore introduced to enable the identification of only those SSLs that were relevant to the scale of process being studied, for example from ocean basin scale (large SSL_{min}) down to krill swarms (small SSL_{min}: Watkins *et al.* 1990). In spite of this precaution, the natural variation within the data still sometimes produced SSLs. These incorrectly identified SSLs, termed 'phantom SSLs' (Fig. 3), were removed in post-processing (section 'SSLEM Validation') by analysis of SSL signal-to-noise ratios; SSLs were removed where the mean SSL MVBS (signal) was smaller than the maximum background MVBS value (noise) by analysing the pixels immediately surrounding the layers.

Separation of merged SSLs

The SSL pixels identified in Section 'Identification of SSLs' were used to generate an SSL mask (Fig. 4b) that bounded pixels that were connected, termed SSL features. These features were not classified as SSLs at this point, as a single feature could consist of several merged SSLs.

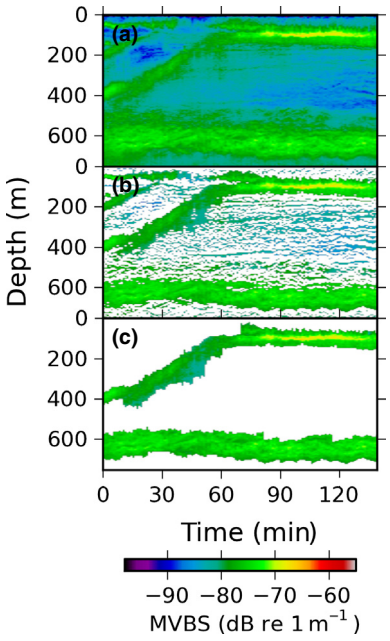

Fig. 4. Processed acoustic image from FV *Austral Leader II* transect during May 2012, where SSL_{min}, the minimum horizontal resolution of sound scattering layers (SSLs), was set to 60 min. (a) Original acoustic image at a resolution of 5 m in depth and 1 min in time. (b) Masked image: only pixels that are deemed to be potential SSL pixels are shown. (c) SSLs identified after removing features smaller than SSL_{min} and filling SSL internal gaps (that are smaller than SSL_{min}).

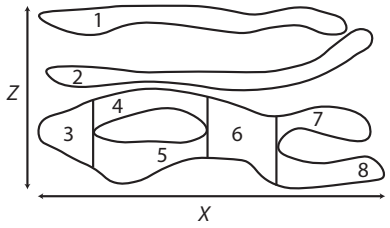

Fig. 5. Segmentation of sound scattering layer (SSL) features into individual SSLs. Each SSL was assigned a unique index value.

Features smaller than SSL_{min} were removed, and internal gaps smaller than SSL_{min} within accepted features were filled (Fig. 4c).

Each feature was then segmented into individual SSLs which existed over a discrete depth range at each point along a time series. This was achieved by implementing a region-based image segmentation process. A simple growing algorithm moved column-by-column through the image, initialising new regions (that would eventually grow into individual SSLs) within features where SSLs merged or split (Fig. 5). SSLs identified in this process that were smaller than SSL_{min} were ignored and not analysed further.

Separation of vertically 'static' and migrant SSLs

Vertically static SSLs were separated from upwardly or downwardly migrating SSLs by application of a change-point analysis (CPA: Page 1954). CPA can detect the existence of multiple trends within a time series by analysing the cumulative deviation from the mean over time. The CPA was conducted using a time series of the mean depth change, ΔZ, over a selected time interval, CPA_{int}, across each SSL (Fig. 6). The

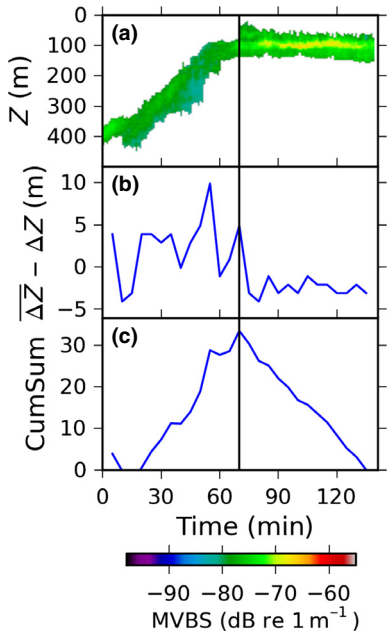

Fig. 6. Change-point analysis of mean sound scattering layer (SSL) depth – SSL taken from the example image in Fig. 4. The vertical black line at 70 min – the maximum point of the cumulative sum of b.) – indicates the point of separation of a static SSL and a migrant SSL. (a) SSL depth. (b) The overall mean depth change of SSL minus each mean depth change in the time series (binned at 6 min intervals) plotted in time. (c) Cumulative sum of b: the maximum value indicates the most significant point of change.

choice of CPA_{int} is related to the size of SSL_{min}. For a relatively large value of SSL_{min} (>4 h for example), a large CPA_{int} value can be chosen and will reduce the likelihood that undulating SSLs, caused by internal waves, would be incorrectly segmented. For small values of SSL_{min}, a CPA_{int} value should be selected to provide enough samples (>10) for the CPA to be conducted appropriately. The deviation of ΔZ from its mean was calculated (Fig. 6b), followed by the cumulative sum of this deviation (Fig. 6c), the most significant point of change was indicated by the largest absolute value (Fig. 6c – black line) and quantified by the range, CPA_{max}, of the cumulative sum values. A confidence interval (CI) was calculated by determining the percentage of 1000 bootstrapped samples of ΔZ that yielded a CPA_{max} value smaller than the original CPA_{max} value. Where a significant change occurred (95% CI), indicating that a SSL changed from simply varying in depth around a static mean to exhibit migrant behaviour (increasing/decreasing depth), SSLs were separated into migrant and static components (Fig. 6).

The CPA was conducted iteratively, until no further statistically significant change (95% CI) within an image segment could be detected: this ensured that multiple migrations, during a diel cycle for example, would all be separated. Multiple migrations were unlikely to occur in this study since at an earlier stage, we partitioned the data into separate day and night segments.

SSL metrics

For each individual SSL identified, a set of SSL metrics were evaluated (Table 1). The depth, duration, MVBS, MVBS standard deviation, MVBS range and layer thickness described spatial extent and backscatter distribution. The vertical velocity and depth range were used to identify and describe migratory layers. The background noise level (BNL) was used to quantify the maximum level of noise surrounding

Table 1. Sound scattering layer (SSL) metrics: summary metrics for individual SSLs. The unit dB re 1 m^{-1} represents 10 times the log base 10 value of a variable with units of m^{-1}; in this case, the mean volume backscattering coefficient (Simmonds & MacLennan 2005) that is relative to a reference level of 1 m^{-1}

SSL metric	Definition	Unit
Depth	Mean depth	m
Depth range	Max (depth)– Min(depth)	m
MVBS	MVBS over entire SSL	dB re 1 m^{-1}
MVBS range	Max(MVBS)– Min(MVBS)	dB re 1 m^{-1}
MVBS STD	Standard deviation of MVBS	dB re 1 m^{-1}
Thickness	Mean SSL thickness	m
Vertical velocity	(change in depth)/time	ms^{-1}
Background Noise Level (BNL)	Max (MVBS) of background pixels surrounding SSL	dB re 1 m^{-1}
Duration	Length of SSL duration	(H:M:S)

the SSL. The maximum value was taken to ensure that it would be greater than the mean MVBS value of SSLs consistent of natural variation within the data (phantom SSLs: section 'Phantom SSLs and SSL_{min}').

The SSL metrics were analysed (see Results 'SSL Metrics') to gain better insight into the nature of SSLs within the study region, enabling inferences concerning the pelagic community (spatial arrangement, distribution and heterogeneity) to be made.

VALIDATION FRAMEWORK

In order to examine the efficacy of our automated SSL identification technique versus the principal present approach, adopted by most acoustic-trawl surveys when assessing fish stocks – visual scrutinisation (which may be subjective and prone to between-operator inconsistencies) – we designed a validation framework to examine potential differences between SSLs determined by the SSLEM and visually scrutinised acoustic images. If visual scrutiny gave highly variable results, this would illustrate the difficulty likely to be encountered in comparative studies and the requirement of an automated method.

The validation was conducted using a subset of the IMOS data. Images from this subset were published online at www.soundscatteringlayers.com. Independent visual scrutiny was performed autonomously by a group of eight students, 50% of whom had attended an acoustic data collection and processing summer school (www.depts.washington.edu/fhl/). Each student estimated 3 SSL metrics, namely the depth, MVBS and thickness for all SSLs they could identify that persisted for a time period longer than 1 hour. Each student considered 10 images selected randomly from a set of 50. The results of the visual scrutiny were compared to those from SSLEM (see Results 'SSLEM Validation').

Results

Sound scattering layers (SSLs) that persisted for time periods longer than 1 h (SSL_{min} = 60 min; CPA_{int} = 6 min: see sections 'Phantom SSLs and SSL_{min}' and 'Separation of vertically 'static' and migrant SSLs' respectively for definitions) were identified and extracted from the IMOS data set (section 'Acoustic data') using the SSL extraction method (SSLEM). SSLs were extracted at these setting in order to conduct a regional analysis of the study area, ensuring that only persistent and therefore characteristic SSLs were identified. In total, 2064 SSLs were extracted from 264 images that were on average 3·4 h in length; an example of the identification of SSLs for an IMOS image is given in Fig. 4. One hundred and eight phantom SSLs (see section 'Phantom SSLs and SSL_{min}') that were identified in the validation procedure were removed. For each SSL, SSL metrics described in 'SSL metrics' were determined and relationships found between select SSL metrics explored (Results 'SSL Metrics').

SSLEM VALIDATION

SSL metrics that were estimated by the students from SSLs visually identified were mapped back on to the original acoustic images for comparison with the SSLEM identified SSLs. Each visually identified SSL was categorised as being a valid/invalid SSL identification. This process was mirrored using the output from the SSLEM, where phantom SSLs (see section 'Phantom SSLs and SSL_{min}') were visually identified after extraction and deemed to be invalid SSLs comprised of background noise. The students identified 211 SSLs from 80 images. For the same SSLs that were identified by more than six of the students from the same image, mean ranges of the estimated metrics were calculated (Table 2).

Of the three SSL identification fields in Table 2 (< SSL_{min}, Noise & TVG), the time-varied gain (TVG) field contained the largest proportion of the students misclassification of SSLs. The TVG increases the amplitude, as a function of time (or depth for a fixed sound speed) of the echo return and serves to amplify both signal, when organisms are present, and the background in an empty pixel, which appears in the acoustic image as depth-dependent noise (Simmonds & MacLennan 2005). This essentially limits the useful (range over which signal dominates noise) range of the instrument and causes visible, layer-like bands to form at the far extent of this range. These layers can resemble SSLs to the untrained eye, but not to the SSLEM; normally, TVG is removed in pre-processing but can just as easily be removed afterwards (Watkins & Brierley 1996).

The SSLEM identified, on average, over 3 times the number of SSLs per acoustic image than the group of students. Whereas the SSLEM output included no variance between repeat identifications and characterisations of SSLs from the same image, the overall mean standard deviation of the number of SSLs identified per image for the students was 0·54. This is in fact quite low and demonstrates that although the students identified fewer SSLs, the group broadly did agree on the number of SSLs per image. Metric estimates by the students were, however, notably large, especially the mean MVBS range (4·8 dB re 1 m^{-1}) that is equivalent to a factor 3 change in the linear domain. The SSLs identified by the SSLEM were also much more likely to be valid (94·8%), that is not phantom SSLs, than those identified by the students (only 75·4% valid), who misidentified SSLs a quarter of the time (Table 2). The SSLEM extracted a total of 108 incorrect SSLs, all of which were considered to be phantom SSLs (section 'Phantom SSLs and SSL_{min}').

Table 2. Summary of method output versus visual scrutiny for identification of sound scattering layers (SSLs)

Method	Mean depth range (m)	Mean MVBS range (dB re 1 m^{-1})	Mean thickness range (m)	< SSL_{min} (%)	Noise (%)	TVG (%)	Valid (%)	Invalid (%)
SSLEM	0	0	0	0	5·2	0	94·8	5·2
VISUAL	26·3	4·8	53	5·7	8·5	10·4	75·4	24·6

Columns definitions from left to right: Method – method of SSL identification; Mean depth range, Mean MVBS range & Mean thickness range – mean ranges of values for the depth, MVBS and thickness metrics for repeat estimations of the same SSLs; < SSL_{min} – percentage of SSLs identified smaller than the pre-set minimum value; Noise – percentage of SSLs consistent of background noise (including phantom SSLs); TVG – percentage of SSLs made up of 'layer-like' noise bands amplified by time-varied gain (TVG); Valid – number of correctly identified SSLs; Invalid – number of incorrectly identified SSLs. Percentages and means are to 1 d.p.

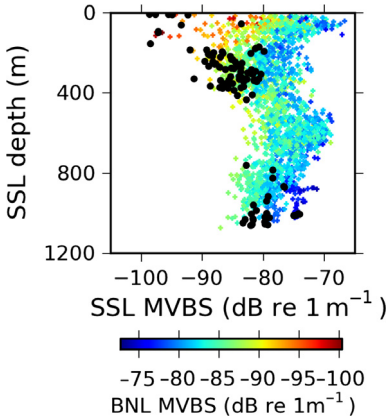

Fig. 7. Background noise level (BNL) for sound scattering layers (SSLs) extracted from the IMOS data set by SSL depth and MVBS. Black points represent phantom SSLs (incorrectly assigned SSLs) identified where BNL > SSL MVBS.

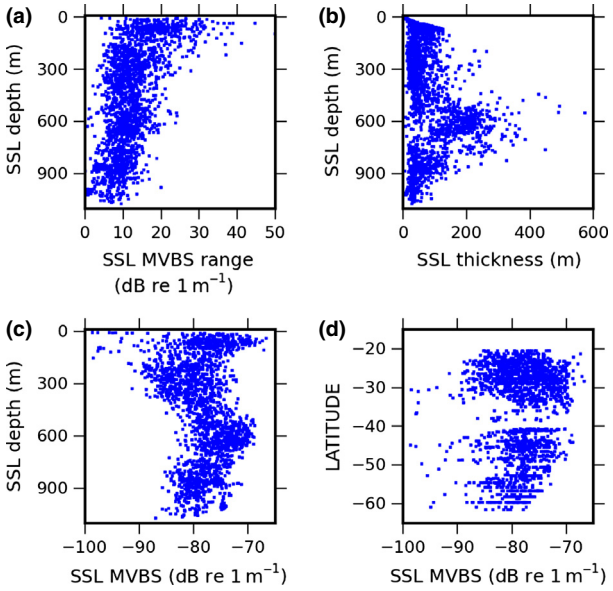

Fig. 8. Sound scattering layer (SSL) metrics extracted from the IMOS data set. (a) Water-column heterogeneity: MVBS range serves as a proxy for biological complexity. (b) SSL thickness as a function of depth. (c) Depth distribution of MVBS. (d) Latitudinal distribution of MVBS.

Phantom SSLs form by the naturally occurring variation in the data. They are an artefact of the SSLEM and hence not detected by visual scrutinisation. This variability is of no consequence within SSLs, but can cause false SSL identification outside (i.e. in empty water – Fig. 3). In order to remove phantom SSLs, the background noise level (BNL) metric was used to identify SSLs that had low signal-to-noise ratios or more accurately, low BNL-to-MVBS ratios. SSLs that had a MVBS value that was smaller than the BNL were identified as being phantom SSLs (black points in Fig. 7). Removing these SSLs from the results increased the validity of the automated method, for the data analysed in this study, to 100%.

Phantom SSLs are apparent throughout the entire water column, except for the region between 400 and 800 m. In this depth region within the study location of the south-west Indian Ocean and Tasman Sea, strong and broad SSLs were persistently present (Fig. 8), meaning that SSLs dominated, excluding the possibility of phantom SSLs forming at the same depth.

SSL METRICS

The SSLEM output a total of 1956 valid (non-phantom) SSLs from the IMOS data. Each SSL was summarised by a set of 9 SSL metrics (Table 1).

Physical characteristics of SSLs provide biological/ecological insight into pelagic community dynamics. For example, the MVBS range increased towards the surface (Fig. 8a) suggesting that the biological community becomes more complex/heterogeneous in the epipelagic region; this could be caused by an increase in species diversity or a larger range of the orientations of organisms, caused by feeding for example. The broadest SSLs lie within the central portion of the mesopelagic region of the water column (Fig. 8b). The highest MVBS values (a proxy for increased biomass/abundance) occurred within the water column at depths of around 600 m and at the surface (Fig. 8c) and also geographically towards 40 degrees south (Fig. 8d). This is consistent with the fact that the zone is the highly productive subtropical convergence zone (see Fig. 1; as identified by Longhurst 1998) where previous work has revealed an enhanced prey field (Boersch-Supan *et al.* 2012).

Discussion

SOUND SCATTERING LAYER EXTRACTION METHOD

The sound scattering layer (SSL) extraction method (SSLEM) was demonstrated here using data observed at a single

frequency, 38 kHz. However, the method is independent of frequency and is entirely appropriate for use with other frequencies. The main differences that would occur would be subject to the characteristics of the incident frequency, for example, reduced depth range and increased resolution at higher frequencies (Simmonds & MacLennan 2005).

The efficacy of the SSLEM was examined by comparing output from that of visually scrutinised data (Table 2). The comparison demonstrated that the SSLEM method is more effective at identifying SSLs (section 'SSLEM Validation'). Visually scrutinised images were subject to SSL misclassification, under classification and sample variation, whereas the SSLEM output was perfectly repeatable, with zero variance between repeat extractions of SSLs and metrics.

Merged vertically static and migrant SSLs were separated by an application of a change-point analysis (Section 'Separation of vertically 'static' and migrant SSLs'). Analysis of the derived SSL metrics revealed water column and geographical trends (Fig. 8). Summarising these data into discrete metrics offers a method of standardised analysis for assessing variability in biological communities in the water column. Importantly, acoustic survey data can now be condensed down from millions of values to a set of community descriptors that can be easily stored, shared and analysed.

SSLEM APPLICATIONS

Analysis of the ocean's SSLs will enable the study of the ocean's mid-trophic structure, providing a global prey field that would be invaluable to predator–prey ecologists. SSL depths could be used to gauge energy expenditure of diving mammals (Boersch-Supan *et al*. 2012; Walters *et al*. 2014), and spatial arrangements of prey fields that could be incorporated into existing biophysical models (for example, SEPODYM: Bertignac, Lehodey & Hampton 1998; Lehodey *et al*. 1998). Monitoring the structure of SSLs over long time periods could reveal climatic influences and the knock-on effects for SSL inhabitants (Lehodey, Chai & Hampton 2003). Spatially distinct formations of SSLs made up of diverse communities are likely to be distinguished and characterised by SSL metrics, allowing the division of regionally distinct biological communities (Longhurst 1998). Whilst the SSLEM does not resolve communities at the species level, such as the Species Identification Methods from Acoustic Multifrequency Information (SIMFAMI: Gajate *et al*. 2004) project, the SSLEM offers an alternate and simpler approach for fisheries and conservation management regimes to assess and monitor open ocean ecosystem health and stability (Korneliussen *et al*. 2008; Handegard *et al*. 2013).

SUMMARY

The SSLEM presented here is directly applicable to all acoustic images, including echograms output from acoustic Doppler current profilers (ADCPs), because it is independent of frequency and scale. Furthermore, it naturally lends itself to more complex multifrequency analysis (Jarvis *et al*. 2010). Unlike other methods (e.g. Cade & Benoit-Bird 2014), the SSLEM was built to facilitate automated processing of data in a standardised fashion that would vary only with consideration of the resolution and scale of the study in mind. It is our hope that its introduction will enable the analysis of a wealth of data that is immediately available, offering insights into the biological structure of the world's ocean. The derived SSL metrics provide a means to summarise the extracted layers, making them readily available for a wide range of analysis. Importantly, the SSLEM offers the opportunity to study the structure of the mid-trophic communities in the ocean and will aid in improving our understanding of an ocean ecosystem.

Acknowledgements

We would like to give special thanks to the reviewers for some very helpful and instructive comments. We would also like to acknowledge the help of the Integrated Marine Observing System data centre (IMOS) and Rick Towler of NOAA for providing vital code for the pre-processing of the acoustic data. Finally, we would like to give thanks to the students, namely Katie Kirk, Katie Wurtzell and Laura Hobbs whom attended the Marine Bioacoustics workshop in Friday Harbor, Marta D'Elia from the Florida International University and Sam Gordine, Mirko Semler, Chris Mueller & Moritz Wiesel from the University of St Andrews, for taking the time to help with the validation of the method.

Data accessibility

Acoustic data are publicly available via the Integrated Marine Observing System (IMOS) – Bio-Acoustic Ships of Opportunity (BA SOOP) subfacility found using the IMOS Ocean data portal: https://imos.aodn.org.au/imos123/home

References

Ainslie, M.A. & McColm, J.G. (1998) A simplified formula for viscous and chemical absorption in seawater. *Journal of the Acoustical Society of America*, **103**, 1671–1672.

Anderson, C.I.H., Brierley, A.S. & Armstrong, F. (2004) Spatio-temporal variability in the distribution of epi- and meso-pelagic acoustic backscatter in the Irminger Sea, North Atlantic, with implications for predation on *Calanus finmarchicus*. *Marine Biology*, **146**, 1177–1188.

Andreeva, I.B., Galybin, N.N. & Tarasov, L.L. (2000) Vertical structure of the acoustic characteristics of deep scattering layers in the ocean. *Acoustical Physics*, **46**, 505–510.

Brierley, A.S. (2014) Quick Guide: diel Vertical Migration. *Current Biology*, **24**, 1074–1076.

Barange, M., Hampton, I., Pillar, S.C. & Soule, M.A. (1994) Determination of composition and vertical structure of fish communities using in situ measurements of acoustic target strength. *Canadian Journal of Fisheries and Aquatic Sciences*, **51**, 99–109.

Berge, J., Cottier, F., Varpe, Ø., Renaud, P.E., Falk-Petersen, S., Kwasniewski, S. *et al*. (2014) Arctic complexity: a case study on diel vertical migration of zooplankton. *Journal of Plankton Research*, **36**, 1279–1297.

Bertignac, M., Lehodey, P. & Hampton, J. (1998) A spatial population dynamics simulation model of tropical tunas using a habitat index based on environmental parameters. *Fisheries Oceanography*, **7**, 326–334.

Bianchi, D., Stock, C., Galbraith, E.D. & Sarmiento, J.L. (2013) Diel Vertical Migration: ecological controls and impacts on the biological pump in a one-dimensional ocean model. *Global Biogeochemical Cycles*, **27**, 478–491.

Bierregaard, R.O., Lovejoy, T.E., Kapos, V., dos Santos, A.A. & Hutchings, R.W. (1992) The biological dynamics of tropical rainforest fragments. *BioScience*, **42**, 859–866.

Boersch-Supan, P., Boehme, L., Read, J., Rogers, A. & Brierley, A. (2012) Elephant seal foraging dives track prey distribution, not temperature: Comment on McIntyre et al. (2011). *Marine Ecology Progress Series*, **461**, 293–298.

Cade, D.E. & Benoit-Bird, K.J. (2014) An automatic and quantitative approach to the detection and tracking of acoustic scattering layers. *Limnology and Oceanography: Methods*, **12**, 742–756.

Chapman, R., Bluy, O., Adlington, R. & Robison, A. (1974) Deep scattering layer spectra in the Atlantic and Pacific Oceans and adjacent seas. *Journal of the Acoustical Society of America*, **56**, 1722–1734.

Coetzee, J. (2000) Use of a shoal analysis and patch estimation system (SHAPES) to characterise sardine schools. *Aquatic Living Resources*, **13**, 1–10.

Gajate, J., Ponce, R., Peña, M., Iglesias, M., Fernandes, P. & Alvarez, F. (2004). The SIMFAMI database: a library of ground truthed acoustic survey data. *Annual Science ICES Conference, ICES ASC*.

Godø, O.R., Samuelsen, A., Macaulay, G.J., Patel, R., Hjøllo, S.S., Horne, J., Kaartvedt, S. & Johannessen, J.A. (2012) Mesoscale eddies are oases for higher trophic marine life. *PLoS ONE*, **7**, e30161.

Handegard, N.O., du Buisson, L., Brehmer, P., Chalmers, S.J., Robertis, A., Huse, G. *et al*. (2013) Towards an acoustic-based coupled observation and modelling system for monitoring and predicting ecosystem dynamics of the open ocean. *Fish and Fisheries*, **14**, 605–615.

Hays, G.C. (2003) A review of the adaptive significance and ecosystem consequences of zooplankton diel vertical migrations. *Hydrobiologia*, **503**, 163–170.

Holliday, D.V., Donaghay, P.L., Greenlaw, C.F., Mcgehee, D.E., Mcmanus, M.M., Sullivan, J.M. & Miksis, J.L. (2003) Advances in defining fine- and micro-scale pattern in marine plankton. *Aquatic Living Resources*, **16**, 131–136.

IMOS (2013) IMOS BASOOP sub-facility, imos.org.au [accessed 1st June 2013].

Irigoien, X., Klevjer, T.A., Røstad, A., Martinez, U., Boyra, G., Acuña, J.L. *et al*. (2014) Large mesopelagic fishes biomass and trophic efficiency in the open ocean. *Nature Communications*, **5**, 3271.

Jarvis, T., Kelly, N., Kawaguchi, S., van Wijk, E. & Nicol, S. (2010) Acoustic characterisation of the broad-scale distribution and abundance of Antarctic krill (*Euphausia superba*) off East Antarctica (30-80°E) in January-March 2006. *Deep Sea Research Part II: Topical Studies in Oceanography*, **57**, 916–933.

Kawaguchi, S., Nicol, S., Virtue, P., Davenport, S.R., Casper, R., Swadling, K.M. & Hosie, G.W. (2010) Krill demography and large-scale distribution in the Western Indian Ocean sector of the Southern Ocean (CCAMLR Division 58.4.2) in Austral summer of 2006. *Deep Sea Research Part II: Topical Studies in Oceanography*, **57**, 934–947.

Kloser, R.J., Ryan, T.E., Young, J.W. & Lewis, M.E. (2009) Acoustic observations of micronekton fish on the scale of an ocean basin : potential and challenges. *ICES Journal of Marine Science*, **66**, 998–1006.

Korneliussen, R.J., Diner, N., Ona, E., Berger, L. & Fernandes, P.G. (2008) Proposals for the collection of multifrequency acoustic data. *ICES Journal of Marine Science*, **65**, 982–994.

Lawson, G. (2001) Species identification of pelagic fish schools on the South African continental shelf using acoustic descriptors and ancillary information. *ICES Journal of Marine Science*, **58**, 275–287.

Lehodey, P., Andre, J.M., Bertignac, M., Hampton, J., Stoens, A., Menkès, C., Memery, L. & Grima, N. (1998) Predicting skipjack tuna forage distributions in the equatorial Pacific using a coupled dynamical bio-geochemical model. *Fisheries Oceanography*, **7**, 317–325.

Lehodey, P., Chai, F. & Hampton, J. (2003) Modelling climate-related variability of tuna populations from a coupled ocean–biogeochemical-populations dynamics model. *Fisheries Oceanography*, **12**, 483–494.

Lehodey, P., Murtugudde, R. & Senina, I. (2010) Bridging the gap from ocean models to population dynamics of large marine predators: a model of mid- trophic functional groups. *Progress in Oceanography*, **84**, 69–84.

Longhurst, A. (1998) *Ecological Geography of the Sea*. Academic Press, San Diego.

Malhi, Y., Phillips, O.L., Lloyd, J., Baker, T., Wright, J., Almeida, S. *et al*. (2002) An international network to monitor the structure, composition and dynamics of Amazonian forests (RAINFOR). *Journal of Vegetation Science*, **13**, 439–450.

McManus, M.A., Alldredge, A.L., Barnard, A.H., Boss, E., Case, J.F., Cowles, T.J. *et al*. (2003) Characteristics, distribution and persistence of thin layers over a 48 hour period. *Marine Ecology Progress Series*, **261**, 1–19.

McManus, M., Cheriton, O., Drake, P., Holliday, D., Storlazzi, C., Donaghay, P. & Greenlaw, C. (2005) Effects of physical processes on structure and transport of thin zooplankton layers in the coastal ocean. *Marine Ecology Progress Series*, **301**, 199–215.

Nicol, S., Pauly, T., Bindoff, N., Wright, S., Thiele, D., Hosie, G.W., Strutton, P.G. & Woehler, E. (2000) Ocean circulation off east Antarctica affects ecosystem structure and sea-ice extent. *Nature*, **406**, 504–507.

Reid, D.G. & Simmonds, E.J. (1993) Image analysis techniques for the study of fish school structure from acoustic survey data. *Canadian Journal of Fisheries and Aquatic Sciences*, **50**, 886–893.

Reid, D.G. (ed.) (2000) Report on echo trace classification. *ICES Cooperative Research Report*, **238**, 1–115.

Simmonds, E.J. & MacLennan, D.N. (2005) *Fisheries Acoustics: Theory and Practice*, 2nd edn. Blackwell Publishing, Oxford, 456 pp.

Page, E.S. (1954) Continuous inspection schemes. *Biometrika*, **41**, 100–115.

Tarasov, L.L. (2002) Deep scattering layers in the northwestern pacific. *Acoustical Physics*, **48**, 81–86.

Walters, A., Lea, M.A., van den Hoff, J., Field, I.C., Virtue, P., Sokolov, S., Pinkerton, M.H. & Hindell, M.A. (2014) Spatially Explicit Estimates of Prey Consumption Reveal a New Krill Predator in the Southern Ocean. *PLoS ONE*, **9**, e86452.

Watkins, J.L., Morris, D.J., Ricketts, C. & Murray, A.W.A. (1990) Sampling biological characteristics of krill: effect of heterogeneous nature of swarms. *Marine Biology*, **107**, 409–415.

Watkins, J.L. & Brierley, A.S. (1996) A post-processing technique to remove background noise from echo integration data. *ICES Journal of Marine Science*, **53**, 339–344.

Wilson, E.O. (1994) Biodiversity: challenge, science, opportunity. *American Zoologist*, **34**, 5–11.

Received 10 March 2015; accepted 10 April 2015
Handling Editor: Andrew Tatem